Intrinsic Charge Dynamics in High-T_c AFeAs(O,F) Superconductors

A. Charnukha,[1,2,3,*] D. Pröpper,[3] N. D. Zhigadlo,[4,5] M. Naito,[6] M. Schmidt,[7] Zhe Wang,[7,†] J. Deisenhofer,[7] A. Loidl,[7] B. Keimer,[3] A. V. Boris,[3] and D. N. Basov[1,8]

[1]*Physics Department, University of California-San Diego, La Jolla, California 92093, USA*
[2]*Leibniz Institute for Solid State and Materials Research, IFW, 01069 Dresden, Germany*
[3]*Max Planck Institute for Solid State Research, 70569 Stuttgart, Germany*
[4]*Laboratory for Solid State Physics, ETH Zurich, CH-8093 Zurich, Switzerland*
[5]*Department of Chemistry and Biochemistry, University of Bern, Freiestrasse 3, CH-3012 Bern, Switzerland*
[6]*Department of Applied Physics, Tokyo University of Agriculture and Technology, Koganei, Tokyo 184-8588, Japan*
[7]*Experimental Physics V, Center for Electronic Correlations and Magnetism, Institute of Physics, University of Augsburg, D-86159 Augsburg, Germany*
[8]*Department of Physics, Columbia University, New York, New York 10027, USA*

(Received 4 July 2017; published 23 February 2018)

We report the first determination of the in-plane complex optical conductivity of 1111 high-T_c superconducting iron oxypnictide single crystals PrFeAs(O,F) and thin films SmFeAs(O,F) by means of conventional and microfocused infrared spectroscopy, ellipsometry, and time-domain THz transmission spectroscopy. A strong itinerant contribution is found to exhibit a dramatic difference in coherence between the crystal and the film. Using extensive temperature-dependent measurements of THz transmission, we identify a previously undetected 2.5-meV collective mode in the optical conductivity of SmFeAs(O,F), which is strongly suppressed at T_c and experiences an anomalous T-linear softening and narrowing below $T^* \approx 110\ \mathrm{K} \gg T_c$. The suppression of the infrared absorption in the superconducting state reveals a large optical superconducting gap with a similar gap ratio $2\Delta/k_B T_c \approx 7$ in both materials, indicating strong pairing.

DOI: 10.1103/PhysRevLett.120.087001

Almost a decade of intensive research into the phenomenology of high-transition-temperature (high-T_c) iron-based superconductors [1] has revealed that the T_c in the vast majority of these compounds is limited to below about 40 K (Ref. [2]). Two notable exceptions to this rule are the oxypnictides of the 1111-type AFeAs(O, F) family (A stands for a rare-earth metal) with T_cs up to about 55 K (Ref. [3]) and the monolayer FeSe grown on $SrTiO_3$ [4–7] with a $T_c \approx 65$ K. It is now clear that in the latter case the abnormally high T_c is afforded not only by the electronic structure and interactions inherent in the iron pnictides and chalcogenides [8–12] but also by additional, extrinsic, interfacial interactions of itinerant carriers in FeSe with the $SrTiO_3$ substrate [13–16]. In the absence of the latter, the maximum T_c attainable in monolayer FeSe was found to only reach the aforementioned limit of ~40 K [6,14,17].

These experimental observations emphasize the uniqueness of the superconducting state in the AFeAs(O, F) materials as they reach the 55-K mark unassisted by extrinsic interactions and hold the key to our understanding of the mechanism of high-T_c superconductivity and further enhancing the superconducting transition temperatures in iron-based compounds. Unfortunately, high-quality single crystals of these materials can only be obtained by a laborious high-pressure growth technique [18,19], which produces microscopic samples. Small linear dimensions and mass effectively bar a large number of bulk-sensitive experimental techniques from contributing to our knowledge base of iron-oxypnictide phenomenology. After several pioneering optical works on polycrystalline 1111-type samples at the dawn of the iron-pnictide research [20–22], few further attempts have been made at determining the intrinsic optical itinerant response of iron oxypnictides within the superconducting FeAs layers and its modification in the superconducting state [23,24]. Another major complication is the polar character of the cleaved crystal planes, which leads to excess charge on the sample surface and makes the interpretation of angle-resolved photoemission spectroscopy (ARPES) as well as scanning-tunneling spectroscopy measurements far from trivial [25–28]. Currently no consensus exists regarding the bulk electronic structure of iron oxypnictides. It is, therefore, imperative to investigate the charge dynamics of these materials and its modification in the superconducting state using a *bulk-sensitive* probe of the electronic structure and interactions.

In this Letter, we report the results of a bulk-sensitive broadband optical-spectroscopy study that overcomes the aforementioned materials-related challenges. We use two complementary approaches to shed first direct light onto the bulk charge-carrier response of iron oxypnictides and its modification in the superconducting state. The first approach employs conventional and microfocused Fourier-transform infrared reflectance spectroscopy as well as microfocused CCD-based spectroscopic ellipsometry to investigate the

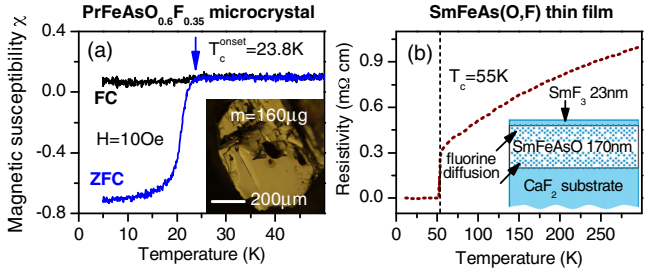

FIG. 1. (a) Temperature dependence of the ac magnetic susceptibility of $PrFeAsO_{0.6}F_{0.35}$ cooled in a zero (blue line) and a 10 Oe (black line) magnetic field, subsequently measured in a 10 Oe field in both cases. The deviation from perfect diamagnetism $\chi = -1$ is due to the geometric factor. Inset: Mass and dimensions of the studied microcrystal. (b) Temperature dependence of the dc resistivity of the optimally doped SmFeAs(O,F) thin film. Inset: Schematic of sample geometry and doping mechanism by fluorine diffusion upon annealing. Additional magnetization measurements substantiating the chemical homogeneity of SmFeAs(O,F) are provided in the Supplemental Material [29].

intrinsic electrodynamics of microscopic high-pressure-grown [18,19] single crystals of $PrFeAsO_{0.6}F_{0.35}$ [nominal composition; see Fig. 1(a)] in a wide spectral range from 15 meV to 6 eV. The second approach employs a unique fluorine-diffusion doping process using *in situ* annealing after growth of parent SmFeAsO thin films synthesized via molecular beam epitaxy on a CaF_2 substrate and capped by a SmF_3 layer [41] [see Fig. 1(b)]. This approach has been shown to result in high-quality optimally doped iron-oxypnictide SmFeAs(O,F) thin films with a maximum $T_c = 55$ K. We have carried out extensive synchrotron- and thermal-source-based spectroscopic ellipsometry as well as time-domain THz transmission spectroscopy measurements on these films in the range from 1 meV to 6.5 eV and at temperatures from 4 to 300 K. These comprehensive measurements allowed us to extract the complex optical conductivity of SmFeAs(O,F) from that of the total response of the multilayer structure and access the itinerant-carrier dynamics in this material down to energies well below those afforded by the linear dimension of microcrystals.

The central observations of our work are summarized in Fig. 2. We find high values of the infrared reflectance in the $PrFeAsO_{0.6}F_{0.35}$ microcrystal [Fig. 2(a)], indicative of a strong itinerant response. By means of a Drude-Lorentz fit [42] we extract the total plasma frequency of 1.4 eV—on par with many other iron-based superconductors [10] despite the extremely singular band structure of the 1111-type materials [27,28]. This itinerant response reaches a high degree of coherence at lowest temperatures (the quasiparticle scattering rate γ has been reliably determined to be about 5 meV, see Supplemental Material [29])—indicating low disorder. Below $T_c = 24$ K the infrared reflectance approaches unity below $E_0 = 28$ meV, indicative of the opening of a nodeless superconducting gap [43,44]. Such a high gapping energy is remarkable for a superconductor with $k_B T_c \approx 2$ meV.

In SmFeAs(O,F), analogous Drude-Lorentz decomposition of the optical conductivity [shaded areas in Fig. 2(b)] reveals an equally strong itinerant response but significantly less coherent [evident from direct comparison with the optical conductivity of the $PrFeAsO_{0.6}F_{0.35}$ microcrystal shown as a dotted line in Fig. 2(b)]. The quasiparticle scattering rate is found to be 150 meV at 300 K and remains unchanged down to lowest temperatures, thus exceeding its $PrFeAsO_{0.6}F_{0.35}$ counterpart by almost 2 orders of magnitude.

By virtue of the large surface area of our SmFeAs(O,F) thin film we were able to investigate its optical response deep in the infrared regime extending to sub-THz frequencies. This spectroscopic access, unprecedented for the 1111-type iron oxypnictides, uncovered the existence of a low-energy collective mode (CM), manifested as a broad peak in the optical conductivity centered at 2.5 meV at

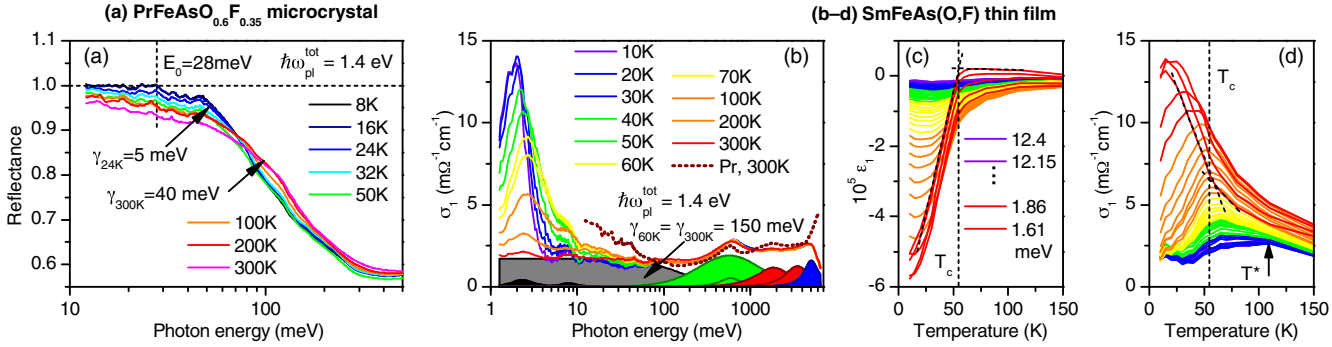

FIG. 2. (a) Temperature dependence of the infrared reflectance of $PrFeAsO_{0.6}F_{0.35}$. Vertical dashed line indicates the energy E_0 at which reflectance reaches unity. (b) Temperature dependence of the optical conductivity of SmFeAs(O,F) (solid lines) compared to that of $PrFeAsO_{0.6}F_{0.35}$ (dotted line). Shaded areas represent the decomposition of the optical conductivity of SmFeAs(O,F) at 300 K into itinerant response (grey shaded area) and interband transitions (green, red, and blue shaded areas) obtained using Drude-Lorentz analysis [42]. Black shaded areas display the contribution of low-energy collective modes to the optical conductivity. (c) Temperature dependence of the real part of the dielectric function at various photon energies as indicated in the panel. Vertical dashed line indicates the T_c determined from the dc resistivity in Fig. 1(b). (d) Temperature dependence of the real part of the optical conductivity at the same photon energies as in panel (c). Additional thermal anomaly is visible at $T = T^*$.

room temperature [left black shaded area in Fig. 2(b)]. The peak narrows and grows dramatically with decreasing temperature, approaching 15 $m\Omega^{-1}$ cm^{-1} at its maximum—an order of magnitude larger than the normal-state dc resistivity values of up to 2 $m\Omega^{-1}$ cm^{-1}. It then rapidly decreases at lower energies to values consistent with the dc transport. Such a CM has not been observed previously in any superconducting iron pnictide or chalcogenide despite significant research effort dedicated to the investigation of their THz properties. Similar CMs in the THz conductivity have, however, been previously identified in other materials with nontrivial electronic properties, including blue bronze ($K_{0.3}MoO_3$), transition-metal chalcogenides, manganese and vanadium oxides, as well as unconventional copper-based superconductors [45–48].

In the superconducting state, we find a strong signature of a coherent superconducting condensate, manifested in the drastic suppression of the real part of the dielectric function in the THz spectral range [Fig. 2(c)]. Optical conductivity in Fig. 2(d) is likewise sensitive to the onset of superconductivity and allows us to extract the superconducting energy gap in what follows. Finally, we discover a distinct temperature scale of $T^* = 110\ \mathrm{K} \gg T_c$ [black arrow in Fig. 2(d)], at which optical conductivity displays an additional thermal anomaly.

The low-energy CM shows dramatic sensitivity to both T_c and T^*. To demonstrate it, we fit the energy dependence of the THz conductivity $\sigma_1(\hbar\omega)$ using two generalized Lorentzians [49–51] on a linear background. The second generalized Lorentzian oscillator peaked around 8 meV is used to improve the overall quality of the fit. Its low intensity does not allow for a reliable extraction of the fit parameters and the determination of its microscopic nature. The fit results are shown in Fig. 3(a) for three representative temperatures. The excellent quality of the fit allows us to extract the Lorentzian parameters for all investigated temperatures with low uncertainty. The temperature dependence of the oscillator strength f_0 [S_j in Eq. (C5) of Ref. [51]], center energy of the mode $\hbar\omega_0$, and the mode width $\hbar\Gamma$ is plotted in Fig. 3(b) and clearly reveals the two characteristic temperatures present in this compound, T_c and T^*. The oscillator strength f_0 shows a dramatic suppression upon entering the superconducting state below 55 K but reveals no strong anomalies near T^*. The mode energy $\hbar\omega_0$ shows the opposite behavior, dropping at T^* with no discernible thermal anomaly at the superconducting transition temperature. The mode width $\hbar\Gamma$ is sensitive to both T_c and T^*.

We hypothesize that the observed CM could originate in the quantum critical fluctuations of incommensurate density-wave order. Density-wave fluctuations or order have been found in both the spin [52,53] and, possibly, charge [54] channel near optimally doped iron-oxypnictide superconductors. The hydrodynamic description of these fluctuations indicates that they should manifest themselves as a low-energy CM in the optical conductivity of strongly

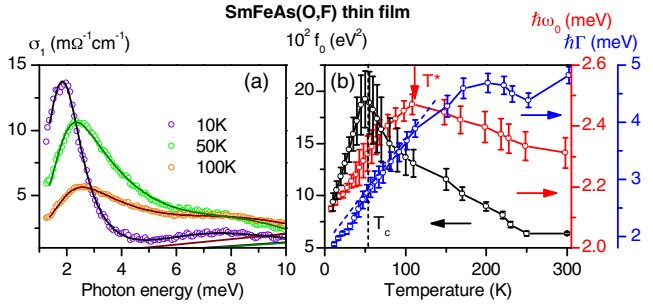

FIG. 3. (a) THz conductivity at three different temperatures revealing the thermal evolution of the CM. Open circles: experimental data; solid lines: fit using two generalized Lorentzians on a linear background. (b) Temperature dependence of the CM oscillator strength f_0 (black symbols and line), energy $\hbar\omega_0$ (red symbols and line), and width $\hbar\Gamma$ (blue symbols and line) extracted from the fit in panel (a). Dashed blue line indicates the linear temperature dependence of $\hbar\Gamma$ between T_c (black dashed line) and T^* (red arrow). Error bars span 1 standard error.

correlated bad metals [48], such as iron-based superconductors [10]. Both the mode energy $\hbar\omega_0$ and width $\hbar\Gamma$ are predicted to exhibit a conspicuous linear temperature dependence, $\hbar\omega_0 \sim \hbar\Gamma \sim k_B T$, analogous to the T-linear dc resistivity observed in many unconventional superconductors [55,56]. Figure 3(b) shows that both $\hbar\omega_0$ and $\hbar\Gamma$ of the CM in SmFeAs(O,F) display a clear linear temperature dependence below T^*, consistent with the aforementioned interpretation. The temperature dependence of the optical conductivity of SmFeAs(O,F) does not support the interpretation of the THz peak as due to Drude-Smith–type backscattering from disorder (see Supplemental Material [29]). Intriguingly, an infrared CM at a somewhat higher energy has been previously identified in the 122-type nonsuperconducting parent compounds [57,58], but its microscopic origin remains to be conclusively established.

Our observation of a T-linear behavior of the THz CM in SmFeAs(O,F) provides first evidence that this phenomenon, pervasive in unconventional superconductors, also occurs in the iron-based superconductors with the highest bulk T_c. It further suggests that detailed investigations of the temperature dependence of the quasiparticle scattering rate in 1111-type microcrystals, similar to previous work on the 122 compounds [59], may reveal a hidden T-linear scaling directly in the itinerant quasiparticle response.

The definitive identification of the nature of the 2.5-meV peak observed here warrants further experimental effort. For instance, we cannot easily distinguish between density-wave CMs in the charge and spin channels because their signatures in optical spectroscopy are qualitatively identical [46,60,61]. Nevertheless, the characteristic time and length scale of this fluctuating order can be estimated based on our measurements. The energy of the mode is about 2.5 meV at 100 K, which corresponds to $\approx 0.3 k_B T$ and an oscillation time scale of 1.6 ps. The corresponding mode line width of about 3.7 meV translates to a characteristic dissipative time

scale of 1.1 ps. The Fermi surface of the 1111-type compounds is highly singular [27,28], but taking a typical electron velocity in the iron pnictides on the order of 10^5 m/s results in the corresponding fluctuation length scale of about 160 nm. We further remark that if the observed 2.5 meV peak is a pinned CM then it corresponds to the phason excitation of the density wave, while the gapped amplitudon excitation does not carry a dipole moment and is expected to be Raman active [46].

In both $PrFeAsO_{0.6}F_{0.35}$ and SmFeAs(O,F) the onset of superconducting coherence is manifested in the transfer of a portion of the infrared spectral weight [hatched areas in Figs. 4(a) and 4(c)] to the dissipationless response at zero frequency according to the Ferrell-Glover-Tinkham sum rule [62]. This spectral weight corresponds directly to the London penetration depth of a superconductor and in our analysis amounts to $\lambda_L^{\mathrm{Pr}} = 190 \pm 100$ nm in $PrFeAsO_{0.6}F_{0.35}$ and a significantly larger $\lambda_L^{\mathrm{Sm}} = 550 \pm 50$ nm in SmFeAs(O,F). The latter was extracted with low uncertainty using a Kramers-Kronig consistency check [63] based on the full

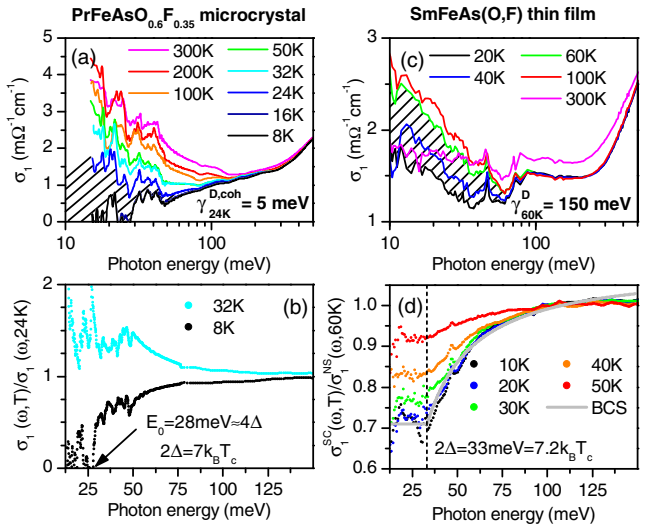

FIG. 4. (a),(c) Temperature dependence of the infrared conductivity of $PrFeAsO_{0.6}F_{0.35}$ and SmFeAs(O,F), respectively. Hatched area indicates the missing spectral weight in the superconducting state that is transferred into the coherent response of the Cooper-pair condensate at zero energy. (b) Photon-energy dependence of the far-infrared conductivity of $PrFeAsO_{0.6}F_{0.35}$ above (32 K, cyan circles) and below (8 K, black circles) T_c normalized to that at 24 K. Black arrow indicates the energy E_0 at which optical absorption is completely suppressed (equivalently, reflectance reaches unity) in the superconducting state. (d) Photon-energy dependence of the far-infrared conductivity of SmFeAs(O,F) at several temperatures in the superconducting state normalized to that in the normal state at 60 K. Vertical dashed line indicates the largest energy of the maximum suppression of the infrared conductivity (consistent with the optical superconducting gap 2Δ in an impure superconductor). Grey line is a fit to the 10 K data using the Mattis-Bardeen expression for the normalized optical conductivity of an impure superconductor in the superconducting state [64].

complex-valued optical conductivity acquired using two phase-sensitive techniques (spectroscopic ellipsometry and time-domain THz transmission spectroscopy).

The signatures of the superconducting optical gap are best revealed in the ratio of the optical conductivity below T_c to that in the normal state just above T_c: $\tilde{\sigma}_1(\omega) = \sigma_1^{\mathrm{SC}}(\omega)/\sigma_1^{\mathrm{NS}}(\omega)$. We examine these ratios for the case of $PrFeAsO_{0.6}F_{0.35}$ and SmFeAs(O,F) in Figs. 4(b) and 4(d), respectively. Corresponding to the near-unity reflectance below E_0 in the superconducting state of $PrFeAsO_{0.6}F_{0.35}$ in Fig. 2(a), $\tilde{\sigma}_1(\omega)$ for this material vanishes below the same energy. In a conventional superconductor with a high impurity concentration, the onset of absorption in the superconducting state occurs when the photon energy is sufficient to dissociate a Cooper pair with the binding energy of 2Δ [43,64]. However, we have demonstrated earlier [see Fig. 2(a) and the corresponding discussion in the text], that $PrFeAsO_{0.6}F_{0.35}$ exhibits a high degree of coherence at low temperatures. In such a clean superconductor, the direct dissociation of a Cooper pair by an incident photon in a two-body process is forbidden by the conservation of energy and momentum. For optical absorption to occur at low temperatures, a quantum of the field mediating the pairing interaction must be excited in addition. If the excitation spectrum of the mediating boson is gapped up to the energy E_g, then absorption becomes allowed above $2\Delta + E_g$ (Ref. [65]). In iron-based superconductors the mediating interaction is believed to be of spin-fluctuation origin and indeed has a gapped excitation spectrum in the superconducting state [2], with the spin-gap energy E_g reaching 2Δ [66,67]. The combination of multiple Andreev reflection spectroscopy [68] and powder inelastic neutron scattering [69] clearly demonstrate that the gap energy in the family of 1111-type materials is $E_g \approx 2\Delta$. Therefore, optical absorption in the superconducting state is expected to occur at an energy of $2\Delta + E_g \approx 4\Delta$, which in the present case results in $\Delta \approx 7$ meV and a gap ratio of $2\Delta/k_B T_c \approx 7$, in a good agreement with the largest values found in the pnictides in general [2] and, more importantly, in the materials of the same family via ARPES [27]. Signatures of boson-assisted absorption in the infrared conductivity have been previously identified in $Ba_{0.68}K_{0.32}Fe_2As_2$, $BaFe_2(As_{0.67}P_{0.33})_2$, and $NaFe_{0.978}Co_{0.022}As$ in Refs. [42,67,70], respectively.

Similarly to the case of $PrFeAsO_{0.6}F_{0.35}$, $\tilde{\sigma}_1(\omega)$ below T_c in SmFeAs(O,F) reveals a plateau below an energy of about 33 meV [see Fig. 4(d)], albeit the absorption does not vanish completely at any photon energy and a sizable residual optical conductivity is present. This observation is consistent with the previous steady-state and ultrafast spectroscopy measurements on 1111-type single crystals and thin films [23,24]. The relatively sharp diamagnetic response in the superconducting state shown in the Supplemental Material [29] as well as the absence of any signature of the 140 K antiferromagnetic transition temperature of the parent SmFeAsO phase [52,71–73] in the dc resistivity shown in

Fig. 1(b) and the CM properties plotted in Fig. 3(b) indicate that this residual conductivity is unlikely to come from inclusions of the parent phase. In the case of SmFeAs(O,F), the significantly less coherent itinerant response than in $PrFeAsO_{0.6}F_{0.35}$ allows for a direct dissociation of the Cooper pairs without the assistance of the mediating boson, as the excess momentum is taken up by the lattice via defects. One may thus expect that the standard Mattis-Bardeen expression for the anomalous skin effect in an impure superconductor with a nodeless gap [64] should apply. Indeed, we find that our experimental data are very well reproduced by this theory [grey line in Fig. 4(d)]. The nodeless character of the superconducting gap is consistent with previous studies of 1111-type compounds [24,27,28,68,74]. The observed agreement between experiment and theory allows us to assign the energy of 33 meV directly to the binding energy of the Cooper pair, 2Δ, which results in a gap ratio $2\Delta/k_BT_c \approx 7.2$. This value is similar to that in $PrFeAsO_{0.6}F_{0.35}$ and, furthermore, to the largest gap ratio identified via ARPES in $NdFeAsO_{1-x}F_x$ (Ref. [27]) and optimally doped $Ba_{0.68}K_{0.32}Fe_2As_2$ (Refs. [63,75]). This commonality suggests a single pairing mechanism in all of these compounds and a strong coupling between electrons and the pairing boson. Our work paves the way to future systematic spectroscopic studies of the in-plane infrared charge response of the high-T_c 1111-type iron oxypnictides. Such investigations will enable the extraction of the spectral function of the pairing boson [42,67,76] and its evolution across the phase diagram, shedding light onto the microscopic origin of the highest bulk superconducting transition temperature among the iron-based superconductors.

We would like to thank J. Hilfiker and T. Tiwald at J. A. Woollam Co., Inc., for their help with conventional and microfocused ellipsometry measurements and R. K. Dumas at Quantum Design for assistance with the magnetic susceptibility measurements on single-crystalline $PrFeAsO_{1-x}F_x$. A. C. acknowledges financial support by the Alexander von Humboldt Foundation. Work at the University of California, San Diego, and Columbia University was supported by National Science Foundation Grant No. DMR1609096 and Gordon and Betty Moore Foundation Grant No. GBMF4533. M. N. was supported by Transformative Research Project on Iron Pnictides (TRIP) and Japan Science Technology (JST). Work in Augsburg was partly supported by the Deutsche Forschungsgemeinschaft (DFG) via the Transregional Collaborative Research Center TRR 80.

*acharnukha@ucsd.edu.
†Present address: Institute of Radiation Physics, Helmholtz-Zentrum Dresden-Rossendorf, Bautzner Landstraße 400, 01328 Dresden, Germany.

[1] Y. Kamihara, T. Watanabe, M. Hirano, and H. Hosono, J. Am. Chem. Soc. **130**, 3296 (2008).
[2] D. S. Inosov, J. T. Park, A. Charnukha, Y. Li, A. V. Boris, B. Keimer, and V. Hinkov, Phys. Rev. B **83**, 214520 (2011).
[3] R. Zhi-An, L. Wei, Y. Jie, Y. Wei, S. Xiao-Li, Zheng-Cai, C. Guang-Can, D. Xiao-Li, S. Li-Ling, Z. Fang *et al.*, Chin. Phys. Lett. **25**, 2215 (2008).
[4] S. He, J. He, W. Zhang, L. Zhao, D. Liu, X. Liu, D. Mou, Y. B. Ou, Q. Y. Wang, Z. Li *et al.*, Nat. Mater. **12**, 605 (2013).
[5] Q. Fan, W. H. Zhang, X. Liu, Y. J. Yan, M. Q. Ren, R. Peng, H. C. Xu, B. P. Xie, J. P. Hu, T. Zhang *et al.*, Nat. Phys. **11**, 946 (2015).
[6] J. Shiogai, Y. Ito, T. Mitsuhashi, T. Nojima, and A. Tsukazaki, Nat. Phys. **12**, 42 (2016).
[7] L. Wang, X. Ma, and Q.-K. Xue, Supercond. Sci. Technol. **29**, 123001 (2016).
[8] D. C. Johnston, Adv. Phys. **59**, 803 (2010); M. M. Qazilbash, J. J. Hamlin, R. E. Baumbach, L. Zhang, D. J. Singh, M. B. Maple, and D. N. Basov, Nat. Phys. **5**, 647 (2009); D. N. Basov and A. V. Chubukov, Nat. Phys. **7**, 272 (2011).
[9] P. Richard, T. Sato, K. Nakayama, T. Takahashi, and H. Ding, Rep. Prog. Phys. **74**, 124512 (2011).
[10] A. Charnukha, J. Phys. Condens. Matter **26**, 253203 (2014).
[11] P. Dai, Rev. Mod. Phys. **87**, 855 (2015).
[12] P. Dai, J. Hu, and E. Dagotto, Nat. Phys. **8**, 709 (2012).
[13] J. J. Lee, F. T. Schmitt, R. G. Moore, S. Johnston, Y. T. Cui, W. Li, M. Yi, Z. K. Liu, M. Hashimoto, Y. Zhang *et al.*, Nature (London) **515**, 245 (2014).
[14] S. N. Rebec, T. Jia, C. Zhang, M. Hashimoto, D. H. Lu, R. G. Moore, and Z. X. Shen, Phys. Rev. Lett. **118**, 067002 (2017).
[15] L. Rademaker, Y. Wang, T. Berlijn, and S. Johnston, New J. Phys. **18**, 022001 (2016).
[16] Y. Wang, K. Nakatsukasa, L. Rademaker, T. Berlijn, and S. Johnston, Supercond. Sci. Technol. **29**, 054009 (2016).
[17] Y. Miyata, K. Nakayama, K. Sugawara, T. Sato, and T. Takahashi, Nat. Mater. **14**, 775 (2015).
[18] N. D. Zhigadlo, S. Weyeneth, S. Katrych, P. J. W. Moll, K. Rogacki, S. Bosma, R. Puzniak, J. Karpinski, and B. Batlogg, Phys. Rev. B **86**, 214509 (2012).
[19] N. D. Zhigadlo, J. Cryst. Growth **382**, 75 (2013).
[20] A. Dubroka, K. W. Kim, M. Rössle, V. K. Malik, A. J. Drew, R. H. Liu, G. Wu, X. H. Chen, and C. Bernhard, Phys. Rev. Lett. **101**, 097011 (2008).
[21] J. Dong, H. J. Zhang, G. Xu, Z. Li, G. Li, W. Z. Hu, D. Wu, G. F. Chen, X. Dai, J. L. Luo *et al.*, Europhys. Lett. **83**, 27006 (2008).
[22] A. V. Boris, N. N. Kovaleva, S. S. A. Seo, J. S. Kim, P. Popovich, Y. Matiks, R. K. Kremer, and B. Keimer, Phys. Rev. Lett. **102**, 027001 (2009).
[23] T. Mertelj, P. Kusar, V. V. Kabanov, L. Stojchevska, N. D. Zhigadlo, S. Katrych, Z. Bukowski, J. Karpinski, S. Weyeneth, and D. Mihailovic, Phys. Rev. B **81**, 224504 (2010).
[24] X. Xi, Y. M. Dai, C. C. Homes, M. Kidszun, S. Haindl, and G. L. Carr, Phys. Rev. B **87**, 180509 (2013).
[25] C. Liu, Y. Lee, A. D. Palczewski, J. Q. Yan, T. Kondo, B. N. Harmon, R. W. McCallum, T. A. Lograsso, and A. Kaminski, Phys. Rev. B **82**, 075135 (2010).
[26] L. X. Yang, B. P. Xie, B. Zhou, Y. Zhang, Q. Q. Ge, F. Wu, X. F. Wang, X. H. Chen, and D. L. Feng, J. Am. Chem. Soc. **72**, 460 (2011).
[27] A. Charnukha, D. V. Evtushinsky, C. E. Matt, N. Xu, M. Shi, B. Büchner, N. D. Zhigadlo, B. Batlogg, and S. V. Borisenko, Sci. Rep. **5**, 18273 (2015).

[28] A. Charnukha, S. Thirupathaiah, V. B. Zabolotnyy, B. Büchner, N. D. Zhigadlo, B. Batlogg, A. N. Yaresko, and S. V. Borisenko, Sci. Rep. **5**, 10392 (2015).

[29] See Supplemental Material at http://link.aps.org/supplemental/10.1103/PhysRevLett.120.087001 for additional information regarding sample characterization and data analysis, which includes Refs. [30–40].

[30] I. H. Malitson, Appl. Opt. **2**, 1103 (1963).

[31] G. R. Field and G. R. Wilkinson, Spectrochim. Acta, Part A **29**, 659 (1973).

[32] W.-T. Su, B. Li, D.-Q. Liu, and F.-S. Zhang, Appl. Surf. Sci. **254**, 6967 (2008).

[33] L. J. Lingg, Ph.D. thesis, University of Arizona, 1990.

[34] H. G. Tompkins and E. A. Irene, *Handbook of Ellipsometry* (William Andrew Inc., Norwich, NY, 2005).

[35] P. Yeh, *Optical Waves in Layered Media* (Wiley, New York, 2005).

[36] J. Hao and L. Zhou, Phys. Rev. B **77**, 094201 (2008).

[37] P. W. Anderson, Phys. Rev. **109**, 1492 (1958).

[38] N. V. Smith, Phys. Lett. **26A**, 126 (1968).

[39] N. V. Smith, Phys. Rev. B **64**, 155106 (2001).

[40] T. L. Cocker, D. Baillie, M. Buruma, L. V. Titova, R. D. Sydora, F. Marsiglio, and F. A. Hegmann, Phys. Rev. B **96**, 205439 (2017).

[41] S. Takeda, S. Ueda, S. Takano, A. Yamamoto, and M. Naito, Supercond. Sci. Technol. **25**, 035007 (2012).

[42] A. Charnukha, O. V. Dolgov, A. A. Golubov, Y. Matiks, D. L. Sun, C. T. Lin, B. Keimer, and A. V. Boris, Phys. Rev. B **84**, 174511 (2011).

[43] M. Tinkham, *Introduction To Superconductivity*, 2nd ed. (McGraw-Hill, New York, 1995).

[44] D. N. Basov and T. Timusk, Rev. Mod. Phys. **77**, 721 (2005).

[45] L. Degiorgi and G. Grüner, Phys. Rev. B **44**, 7820 (1991).

[46] G. Grüner, Rev. Mod. Phys. **60**, 1129 (1988).

[47] C.-W. Chen, J. Choe, and E. Morosan, Rep. Prog. Phys. **79**, 084505 (2016).

[48] L. V. Delacrétaz, B. Goutéraux, S. A. Hartnoll, and A. Karlsson, SciPost Phys. **3**, 025 (2017); D. N. Basov, A. V. Puchkov, R. A. Hughes, T. Strach, J. Preston, T. Timusk, D. A. Bonn, R. Liang, and W. N. Hardy, Phys. Rev. B **49**, 12165 (1994); D. N. Basov, B. Dabrowski, and T. Timusk, Phys. Rev. Lett. **81**, 2132 (1998).

[49] J. Humlíček, R. Henn, and M. Cardona, Phys. Rev. B **61**, 14554 (2000).

[50] D. Pröpper, A. N. Yaresko, T. I. Larkin, T. N. Stanislavchuk, A. A. Sirenko, T. Takayama, A. Matsumoto, H. Takagi, B. Keimer, and A. V. Boris, Phys. Rev. Lett. **112**, 087401 (2014).

[51] T. I. Larkin, A. N. Yaresko, D. Pröpper, K. A. Kikoin, Y. F. Lu, T. Takayama, Y. L. Mathis, A. W. Rost, H. Takagi, B. Keimer *et al.*, Phys. Rev. B **95**, 195144 (2017).

[52] A. J. Drew, C. Niedermayer, P. J. Baker, F. L. Pratt, S. J. Blundell, T. Lancaster, R. H. Liu, G. Wu, X. H. Chen, I. Watanabe *et al.*, Nat. Mater. **8**, 310 (2009).

[53] A. J. Drew, F. L. Pratt, T. Lancaster, S. J. Blundell, P. J. Baker, R. H. Liu, G. Wu, X. H. Chen, I. Watanabe, V. K. Malik *et al.*, Phys. Rev. Lett. **101**, 097010 (2008).

[54] A. Martinelli, P. Manfrinetti, A. Provino, A. Genovese, F. Caglieris, G. Lamura, C. Ritter, and M. Putti, Phys. Rev. Lett. **118**, 055701 (2017).

[55] J. A. N. Bruin, H. Sakai, R. S. Perry, and A. P. Mackenzie, Science **339**, 804 (2013).

[56] I. M. Hayes, R. D. McDonald, N. P. Breznay, T. Helm, P. J. W. Moll, M. Wartenbe, A. Shekhter, and J. G. Analytis, Nat. Phys. **12**, 916 (2016).

[57] W. Z. Hu, J. Dong, G. Li, Z. Li, P. Zheng, G. F. Chen, J. L. Luo, and N. L. Wang, Phys. Rev. Lett. **101**, 257005 (2008).

[58] A. Charnukha, D. Pröpper, T. I. Larkin, D. L. Sun, Z. W. Li, C. T. Lin, T. Wolf, B. Keimer, and A. V. Boris, Phys. Rev. Lett. **88**, 184511 (2013).

[59] Y. M. Dai, B. Xu, B. Shen, H. Xiao, H. H. Wen, X. G. Qiu, C. C. Homes, and R. P. S. M. Lobo, Phys. Rev. Lett. **111**, 117001 (2013).

[60] G. Grüner, Rev. Mod. Phys. **66**, 1 (1994).

[61] O. V. Dolgov and M. L. Kulić, Phys. Rev. B **66**, 134510 (2002).

[62] R. A. Ferrell and R. E. Glover, Phys. Rev. **109**, 1398 (1958).

[63] A. Charnukha, P. Popovich, Y. Matiks, D. L. Sun, C. T. Lin, A. N. Yaresko, B. Keimer, and A. V. Boris, Nat. Commun. **2**, 219 (2011).

[64] D. C. Mattis and J. Bardeen, Phys. Rev. **111**, 412 (1958).

[65] E. J. Nicol, J. P. Carbotte, and T. Timusk, Phys. Rev. B **43**, 473 (1991).

[66] C. Zhang, H. F. Li, Y. Song, Y. Su, G. Tan, T. Netherton, C. Redding, S. V. Carr, O. Sobolev, A. Schneidewind *et al.*, Phys. Rev. B **88**, 064504 (2013).

[67] A. Charnukha, K. W. Post, S. Thirupathaiah, D. Pröpper, S. Wurmehl, M. Roslova, I. Morozov, B. Büchner, A. N. Yaresko, A. V. Boris *et al.*, Sci. Rep. **6**, 18620 (2016).

[68] Y. G. Ponomarev, S. A. Kuzmichev, T. E. Kuzmicheva, M. G. Mikheev, M. V. Sudakova, S. N. Tchesnokov, O. S. Volkova, A. N. Vasiliev, V. M. Pudalov, A. V. Sadakov *et al.*, J. Supercond. Novel Magn. **26**, 2867 (2013).

[69] S.-I. Shamoto, M. Ishikado, A. D. Christianson, M. D. Lumsden, S. Wakimoto, K. Kodama, A. Iyo, and M. Arai, Phys. Rev. B **82**, 172508 (2010).

[70] S. J. Moon, A. A. Schafgans, S. Kasahara, T. Shibauchi, T. Terashima, Y. Matsuda, M. A. Tanatar, R. Prozorov, A. Thaler, P. C. Canfield *et al.*, Phys. Rev. Lett. **109**, 027006 (2012).

[71] H. Maeter, J. E. Hamann Borrero, T. Goltz, J. Spehling, A. Kwadrin, A. Kondrat, L. Veyrat, G. Lang, H. J. Grafe, C. Hess *et al.*, arXiv:1210.6959.

[72] A. Martinelli, A. Palenzona, M. Putti, and C. Ferdeghini, Phys. Rev. B **85**, 224534 (2012).

[73] A. Martinelli, A. Palenzona, M. Tropeano, M. Putti, C. Ferdeghini, G. Profeta, and E. Emerich, Phys. Rev. Lett. **106**, 227001 (2011).

[74] T. E. Kuzmicheva, S. A. Kuzmichev, K. S. Pervakov, V. M. Pudalov, and N. D. Zhigadlo, Phys. Rev. B **95**, 094507 (2017).

[75] G. Li, W. Z. Hu, J. Dong, Z. Li, P. Zheng, G. F. Chen, J. L. Luo, and N. L. Wang, Phys. Rev. Lett. **101**, 107004 (2008).

[76] J. P. Carbotte, Rev. Mod. Phys. **62**, 1027 (1990).